

PROJECTIVE REPRESENTATIONS OF HECKE GROUPS FROM TOPOLOGICAL QUANTUM FIELD THEORY

YUZE RUAN

ABSTRACT. We construct projective (unitary) representations of Hecke groups from the vector spaces associated with the Witten-Reshetikhin-Turaev topological quantum field theory of higher genus surfaces. In particular, we generalize the modular data of Temperley-Lieb-Jones modular categories. We also study some properties of the representation. We show the image group of the representation is infinite at low levels in genus 2 by explicit computations. We also show the representation is reducible with at least three irreducible summands when the level equals $4l + 2$ for $l \geq 1$.

1. INTRODUCTION

In 1983, Vaughan Jones discovered a new family of representations of braid groups, from the study of the index of II_1 subfactors [18, 19], which in turn gave a beautiful new invariant for knots, known as the Jones polynomials. Later, Witten in his seminal paper [42] uncovered a deep connection between the Jones polynomial and the Chern-Simons gauge theory. He further provided arguments for constructing $2 + 1$ topological quantum field theory (TQFT) based on it. The first rigorous mathematical construction of TQFT was developed by Reshetikhin and Turaev, using quantum groups $U_q(\mathfrak{sl}_2)$ [32]. A skein theoretical construction was given by Blanchet, Habegger, Masbaum, and Vogel [5, 6] (pioneered by Lickorish [23]). Turaev carried out the most general construction in [36], which employs modular categories as input data.

In essence, a $2 + 1$ TQFT is a symmetric monoidal functor from the cobordism category to the category of modules over some ring (often equipped with additional structure), we denote the module associated to a surface Σ by $V(\Sigma)$, and denote the homomorphism associated to a cobordism M by $Z(M)$. A fascinating feature of TQFTs is their ability to produce projective representations $\text{Mod}(\Sigma) \rightarrow \text{PGL}(V(\Sigma))$ of the mapping class groups $\text{Mod}(\Sigma)$. These representations are known to be asymptotically faithful [13, 1]. In particular, when Σ is an n -punctured disc, the corresponding mapping class group is the braid group B_n , and the representations, derived from $U_q(\mathfrak{sl}_2)$, recover

the Jones representations [19]. For a genus-1 surface, $\text{Mod}(\Sigma)$ is isomorphic to $\text{SL}_2(\mathbb{Z})$. The images of the generators $s = \begin{pmatrix} 0 & -1 \\ 1 & 0 \end{pmatrix}$, $t = \begin{pmatrix} 1 & 1 \\ 0 & 1 \end{pmatrix}$, yield the modular S - and T -matrices, referred as the modular data of the input modular categories. While it is not a complete invariant for modular categories [30], they encode many information and play a crucial role in the classification of the modular categories [34, 8], as well as in the classification of partition functions in the conformal field theory [9]. Moreover, In [31], Ng and Schauenburg demonstrated that the kernel of this representation is a congruence subgroup of $\text{SL}_2(\mathbb{Z})$, in particular, the image is finite.

In this paper, we focus on the skein version of TQFT constructed in [6], or equivalently the TQFT derived from Temperley-Lieb-Jones (TLJ) categories [40], [37, Chapter XII]. We generalize the modular data of TLJ-categories through the mapping class group representation of higher genus surfaces, and we find the representations of Hecke groups $\Gamma_q \in \text{PSL}_2(\mathbb{R})$ ($\tilde{\Gamma}_q \in \text{SL}_2(\mathbb{R})$), which are generated by $t_q = \begin{pmatrix} 1 & 2 \cos(\frac{\pi}{q}) \\ 0 & 1 \end{pmatrix}$, $s = \begin{pmatrix} 0 & -1 \\ 1 & 0 \end{pmatrix}$ ($q \geq 3$), and the image of t_q is a diagonal matrix.

Theorem 1.1. *We have projective (unitary) representations h_r (where r is the level of the theory) of $\tilde{\Gamma}_{2g+1}$ from the TQFT vector spaces $V_r(\Sigma_g)$. In particular, when $g = 1$, $h_r(t_3), h_r(s)$ provides the modular data of TLJ modular categories. When $g = 2$, we define $\mathcal{J} := h_r(s)$ and a diagonal matrix $\mathcal{T}_r := h_r(t_5)$. They satisfy the relations:*

$$(1) \quad \begin{aligned} \mathcal{J}_r^2 &= I, \\ (\mathcal{T}_r \mathcal{J}_r)^5 &= \left(\frac{\mathcal{P}_r^+}{\mathcal{P}_r^-} \right)^2 I. \end{aligned}$$

It's natural to ask the following

Question 1.2. Is the image of h_r finite for $g \geq 2$?

We perform some concrete calculations for the genus-2 case and obtain the following results:

Theorem 1.3. *The group $h_r(\Gamma_5)$ is infinite for $r = 3, 7, 9, 11, 13$.*

And it appears that the trace of certain elements grows exponentially in r . It is known from the result of Funar [14] that if one considers the entire mapping class group, then the image is infinite in almost all cases. Additionally, Masbaum found an infinite

order element [25]. However, their methods cannot directly address our question. The reason is that they used the factorization axiom to cut the surface into smaller pieces, and studied the mapping classes supported on subsurfaces, therefore the problem can be reduced to the calculations of braid group representations. In our case, however, Pseudo-Anosov mapping classes are generic within the corresponding subgroup of the mapping class group. meaning they cannot be supported on any subsurface. We noticed the following conjecture of Andersen, Masbaum and Ueno.

Conjecture 1.4. [2, Conjecture 2.4] *The image of a Pseudo-Anosov mapping class under TQFT representations is of infinite order for all sufficiently large levels.*

If this conjecture holds, it would imply that most of our representations are infinite. Recent progress on this conjecture for higher-genus surfaces with at least two boundary components is discussed in [11], along with its connection to the volume conjecture in [3].

Here is a brief outline of this paper. In Section 2, we review the basic definitions and properties of the Hecke group and the mapping class group. In Section 3, we review Thurston's construction and use it to define an inclusion $\rho : \tilde{\Gamma}_{2g+1} \hookrightarrow \text{Mod}(\Sigma_g)$ with an explicit geometric description of $\rho(s)$. In Section 4, we review the general framework of TQFT and the mapping class group actions. Here, we carefully analyze these actions to prove Theorem 1.1 and perform explicit calculations to establish Theorem 1.3. In Section 5, we examine the reducibility of h_r . By using the spin structures, we conclude that the representation is reducible with at least three irreducible summands when $r = 4l + 2$ for $l \geq 1$.

ACKNOWLEDGEMENT

The author would like to thank Vaughan Jones, this work cannot be done without his constant support, guidance, and encouragement. The author thanks Dietmar Bisch for his constant support at Vanderbilt. The author thanks Spencer Dowdall for helpful discussions and providing the reference [22]. The author thanks Eric Rowell and Yilong Wang for helpful discussions. The author also thanks Zhengwei Liu and BIMSA (Beijing Institute of Mathematics Sciences and Applications) where this work was completed.

2. PRELIMINARIES

2.1. Hecke group. Here we mainly follow the discussion of Hecke groups in [16, Appendix III].

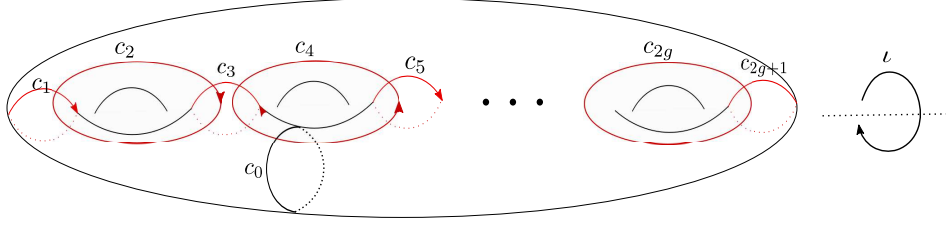


FIGURE 1. Genus g surface with simple closed curves

Definition 2.1.1. *The Hecke group Γ_q ($q \geq 3$, odd) is the subgroup of $\mathrm{PSL}(2, \mathbb{R})$ generated by*

$$A_q = \begin{pmatrix} 1 & \lambda \\ 0 & 1 \end{pmatrix}, \quad B_q = \begin{pmatrix} 1 & 0 \\ -\lambda & 1 \end{pmatrix}. \quad (\lambda = 2 \cos \frac{\pi}{q})$$

Theorem 2.1.2. [16] *Let $J = \begin{pmatrix} 0 & -1 \\ 1 & 0 \end{pmatrix}$, we have $J = A_q^{-1}(A_q B_q)^{\frac{q+1}{2}}$ and*

$$\Gamma_q = \langle J, A_q J \rangle \cong \mathbb{Z}_2 * \mathbb{Z}_q.$$

Moreover, if we view the matrices as elements in $\mathrm{SL}(2, \mathbb{R})$, then

$$(2) \quad J = (A_q B_q)^{\frac{q(q-1)}{2}} A_q^{-1} (A_q B_q)^{\frac{q+1}{2}},$$

*and they generate a group $\tilde{\Gamma}_q$ isomorphic to amalgamate free product $\mathbb{Z}_2 *_{\mathbb{Z}_2} \mathbb{Z}_q$, which has the presentation*

$$\tilde{\Gamma}_q = \langle J, A_q J \rangle \cong \langle s, t \mid s^4 = (ts)^{2q} = 1, s^2 = (ts)^q \rangle.$$

Proof. One can find the proof for the structure of Γ_q in [16, Appendix III] or [10, Chapter II]. The structure for $\tilde{\Gamma}_q$ follows easily from checking the relation and observing $J^2 = (A_q B_q)^q = -I$, $(A_q J)^2 = -A_q B_q$. \square

Remark 2.1.3. When $q = 3$, $\Gamma_q \cong \mathrm{PSL}(2, \mathbb{R})$, $\tilde{\Gamma}_q \cong \mathrm{SL}(2, \mathbb{R})$. When $\lambda \geq 2$, the group is freely generated by those two elements.

2.2. Mapping class group. This section mainly follows [12, 4].

Definition 2.2.1. *Let Σ be a surface possible with punctures and boundaries, and $\mathrm{Homeo}^+(\Sigma, \partial\Sigma)$ be the group of orientation-preserving homeomorphisms of Σ that restrict to the identity on $\partial\Sigma$. The **mapping class group** of Σ , denoted $\mathrm{Mod}(\Sigma)$, is the*

group

$$\text{Mod}(\Sigma) = \text{Homeo}^+(\Sigma, \partial\Sigma)/\text{isotopy} .$$

Definition 2.2.2. Fix a simple closed curve γ on the surface, the **right (left) Dehn twist** about γ , denote by T_γ (resp. T_γ^{-1}), is the isotopy class of a homeomorphism supported in an annular neighborhood U of γ . More precisely, let $\psi : U \rightarrow \mathbb{R}/l_1\mathbb{Z} \times [0, l_2]$ be an orientation preserving homeomorphism, T_γ is given by conjugating ψ with the affine map

$$(x, y) \mapsto (x \pm y \frac{l_1}{l_2}, y) .$$

Where $+$ gives a right (or positive) twist, while $-$ gives a left (or negative) twist.

For now, we consider mainly closed surfaces with no punctures and right Dehn twists, the presentation of the mapping class group is known, for example see[39]. The next proposition gives many interesting properties of Dehn twists, one can see, for example, [12, Chapter 3] for the proofs.

Proposition 2.2.3. Let γ_1, γ_2 be any isotopy classes of simple closed curves in Σ with geometric intersection number $i(\gamma_1, \gamma_2)$. Let $f \in \text{Mod}(\Sigma)$, we have

- (a) $T_{f(\gamma_1)} = fT_{\gamma_1}f^{-1}$,
- (b) $fT_{\gamma_1}^k = T_{\gamma_1}^k f \iff f(\gamma_1) = \gamma_1$,
- (c) $i(\gamma_1, \gamma_2) = 0 \iff T_{\gamma_1}T_{\gamma_2} = T_{\gamma_2}T_{\gamma_1}$.

Theorem 2.2.4 ([12, 39]). Let Σ_g denote genus g closed surface with no punctures, then $\text{Mod}(\Sigma_g)$ is generated by the (left) Dehn twists around curves $c_i (0 \leq i \leq 2g)$ shown in Figure 1. There are relations among generators: the disjoint relation (far commutativity), the braid relation, the chain relation, the lantern relation and the hyperelliptic relation.

Definition 2.2.5 ([12]). Let ι_g be the hyperelliptic involution in Figure 1 and let $S\text{Homeo}^+(\Sigma_g)$ be the centralizer in $\text{Homeo}^+(\Sigma_g)$ of ι_g , i.e.,

$$S\text{Homeo}^+(\Sigma_g) = C_{S\text{Homeo}^+(\Sigma_g)}(\iota_g) .$$

The **symmetric mapping class group**, denoted by $\text{SMod}(\Sigma_g)$, is the group

$$\text{SMod}(\Sigma_g) = S\text{Homeo}^+(\Sigma_g)/\text{isotopy} .$$

Remark 2.2.6. In general, a hyperelliptic involution is an order two mapping class acting on the homology by $-I$, and it is unique up to conjugations when genus ≥ 3 [12, Proposition 7.15]. Here we pick the special ι_g as indicated in Figure 1.

Theorem 2.2.7 (Birman-Hilden Theorem). *For any g , $\text{SMod}(\Sigma_g)/\langle \iota_g \rangle \cong \text{Mod}(S_{0,2g+2})$, where $\text{Mod}(S_{0,2g+2})$ is the mapping class group of $2g+2$ punctured sphere, or the spherical braid group $\pi_1 B_{0,2g+2} S^2$. In particular, $\text{SMod}(\Sigma_g)$ is generated by T_{c_i} ($1 \leq i \leq 2g+1$), they satisfy the relations in the braid group \mathcal{B}_{2g+2} .*

3. HECKE GROUP INSIDE MAPPING CLASS GROUP

3.1. Flat structure and Thurston's construction. [35, 22, 29, 12]

Definition 3.1.1. A **multicurve** $A = \{\alpha_1, \dots, \alpha_n\}$ is a set of pairwise disjoint simple closed curves on the surface, the **multi-twist** with **multiplicity** $p := \{p_1, \dots, p_n\}$ ($p_i \in \mathbb{Z}_+$) about A is a mapping class $T_{A,p} := \prod_{i=1}^n T_{\alpha_i}^{p_i}$. For simplicity, we write $T_A := T_{A,\{1, \dots, 1\}}$.

Definition 3.1.2. A pair of multicurves $A = \{\alpha_1, \dots, \alpha_n\}$, $B = \{\beta_1, \dots, \beta_m\}$ **bind** the surface Σ_g if they meet only at transverse double points, and every component of $\Sigma_g - (A \cup B)$ is a polygonal region with at least 4 sides (running alternately along A and B).

Now view $A \cup B$ as a (bipartite) graph, where the vertexes are given by the simple closed curves in A, B , and two vertexes are connected by n edge iff the corresponding curves have geometric intersection number n . We denote the graph by $\mathcal{G}(A, B)$, and the corresponding adjacency matrix by N , where $N_{i,j} = i(\alpha_i, \beta_j)$. Let $p = \{p_1, \dots, p_n\}$, $q = \{q_1, \dots, q_m\}$ be a pair of multiplicities, we denote the corresponding diagonal matrix by P, Q . If A, B binds Σ_g , then $\mathcal{G}(A, B)$ is connected, hence the matrix $M = \begin{pmatrix} 0 & PN \\ QN^t & 0 \end{pmatrix}$ is primitive, and one can apply the Perron–Frobenius theorem.

We denote the Perron–Frobenius eigenvalue and eigenvector by $\mu_{A,B}^{p,q}, \begin{pmatrix} v_{A,B}^{p,q} \\ v_{A,B}^{p,q} \end{pmatrix}$,

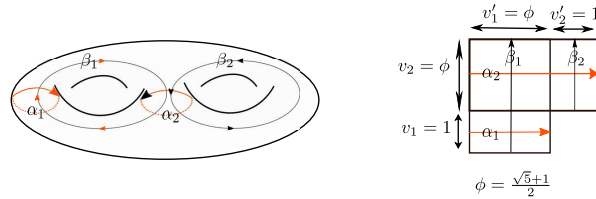


FIGURE 2. A flat structure of genus 2 surfaces where the given multi-twists act affinely.

such that

$$(3) \quad \begin{aligned} PNv_{A,B}^{p,q} &= \mu_{A,B}^{p,q}v_{A,B}^{p,q}, \\ QN^tv_{A,B}^{p,q} &= \mu_{A,B}^{p,q}v_{A,B}^{p,q}. \end{aligned}$$

Given a surface Σ_g , Thurston constructs a certain type of **flat structure** (singular Euclidean structure) on the surface [35], also see [43] for equivalent definitions of the flat structure. Here we will give one arising from polygons.

Definition 3.1.3 ([43]). *A **flat structure** on the surface Σ_g is given by a cell decomposition consisting of a finite union of polygons in \mathbb{C} (Euclidean polygons), with a choice of pairing of parallel sides of equal length. Two sets of polygons are considered to define the same flat structure if one can be cut into pieces along straight lines and these pieces can be translated and re-glued to form the other set of polygons.*

For example Figure 2 gives a flat structure on Σ_2 , where we have one vertex and it is the only 0-cell.

Now given a pair of multi curves A, B binding Σ_g , we construct a flat structure on which the corresponding multi-twists T_A, T_B act affinely.

We assign $\{|\alpha_1|, \dots, |\alpha_n|\} = v_{A,B}^{p,q}$, $\{|\beta_1|, \dots, |\beta_m|\} = v_{A,B}^{p,q}$ to be the length of curves in A, B . Consider the dual cell decomposition of the obvious cell decomposition coming from cutting along the curves in $A \cup B$ (since $A \cup B$ binds Σ_g), the number of 2-cells is equal to the number of nonzero entries in N , and each 2-cells is a rectangle. The length we assign to each 1-cell is equal to the length of the curve intersecting with it, see Figure 2. Using this flat structure we get an action of a pair of multi-twists with multiplicities.

Theorem 3.1.4 (Thurston's construction [29, 35]). *Let $A = \{\alpha_1, \dots, \alpha_n\}$, $B = \{\beta_1 \dots \beta_m\}$ be a pair of multi curves binding the surface Σ_g , and $p = \{p_1, \dots, p_n\}$, $q = \{q_1, \dots, q_m\}$ be a pair of multiplicities. Then we have a representation $\rho_{A,B}^{p,q} : \langle T_{A,p}, T_{B,q} \rangle \rightarrow \text{PSL}(2, \mathbb{R})$ given by*

$$T_{A,p} \mapsto \begin{pmatrix} 1 & \mu_{A,B}^{p,q} \\ 0 & 1 \end{pmatrix}, \quad T_{B,q} \mapsto \begin{pmatrix} 1 & 0 \\ -\mu_{A,B}^{p,q} & 1 \end{pmatrix}.$$

Moreover, the map $\rho_{A,B}^{p,q}$ lifts to $\text{SL}(2, \mathbb{R})$ if and only if the curves in $A \cup B$ can be oriented so that their geometric and algebraic intersection numbers coincide ($\alpha_i \cdot \beta_j = i(\alpha_i, \beta_j)$).

Proof. The curves in A decompose the surface into n copies of cylinders with height vector equal to $v_{A,B}^{p,q}$, and circumference vector equal to $Nv_{A,B}^{p,q}$. It is obvious one can make T_A act affinely when restricted to each cylinder as indicated in Definition 2.2.2. Now from (3) the linear part of the action agrees on all cylinders. The same is true for T_B . Therefore, the derivatives of T_A and T_B give the desired representation. When $\alpha_i \cdot \beta_j = i(\alpha_i, \beta_j)$ for $1 \leq i \leq m$, $1 \leq j \leq n$, we have well-defined horizontal and vertical directions, hence a linear representation. One can see [12, Chapter 14] or [29, Section 4] for more details. \square

When $\mu_{A,B}^{p,q} < 2$, the corresponding graph $\mathcal{G}(A, B)$ and multiplicities are restrictive, one can see [16, Chapter 1.4] for the discussion on the graphs with norm less than 2. When there is no multiplicity, The graphs are of type A, D or E [22]. A few calculations also show if there are multiplicities, then only type A graph appears, with multiplicity two on a 1-valence vertex and the corresponding $\mu_{A,B}^{p,q}$ equals to the norm of the type B Coxeter graph.

Remark 3.1.5. Due to the Nielson-Thurston classification, a mapping class is either periodic, reducible or Pseudo-Anosov. Thurston used this construction to construct the Pseudo-Anosov mapping class [35]. In fact, a mapping class in this construction is periodic, reducible or Pseudo-Anosov if and only if the image under $\rho_{A,B}^{p,q}$ is elliptic, parabolic or hyperbolic (determined by the traces).

The Riemann surfaces equipped with flat structures are called flat surfaces, which can also be described analytically by a pair (X, ω) , where X is a closed Riemann surface, and ω is a holomorphic 1-form on X . One can choose an atlas of X such that ω has the form dz away from zeros for some charts z with transition maps given by translations, and for the neighborhood of a zero ω has the form $w^k dw$ for some charts w . There is natural action of $\mathrm{GL}_2^+(\mathbb{R})$, given by $g(X, \omega) = (Y, g \circ \omega)$, where Y is the Riemann surface such that $g \circ \omega$ is holomorphic on Y . If we consider the flat surfaces in the sense of Definition 3.1.3, then the action is more explicit which is given by actions on polygons in \mathbb{R}^2 . The study of the flat surfaces and their behaviors under the $\mathrm{GL}_2^+(\mathbb{R})$ actions has wide applications in the study of geometry, topology and dynamic systems [44], In particular, by the results of Veech, ([38, 28]), the flat surface obtained by multi curves above has a nontrivial stabilizer group which is a discrete subgroup of $\mathrm{PSL}(2, \mathbb{R})$ (or $\mathrm{SL}(2, \mathbb{R})$) containing the group generated by affine automorphisms given by the multi-twists.

3.2. Relation between two groups.

Proposition 3.2.1. [22] *The representation $\rho_{A,B}^{p,q}$ is faithful when $\mu_{A,B}^{p,q} \geq 2$. When $\mu_{A,B}^{p,q} < 2$, the order of $\ker(\rho_{A,B}^{p,q})$ is at most 2.*

Proof. When $\mu_{A,B}^{p,q} \geq 2$, the image of $\rho_{A,B}^{p,q}$ is a free group on two generators. The injectivity follows from the Hopfian property of the finitely generated free group.

When $\mu_{A,B}^{p,q} < 2$ with no multiplicities, see [22, Theorem 7.3], one has a homomorphism δ from $\ker(\rho_{A,B})$ to the automorphism group of the graph preserving the bicoloring, both the image and kernel are of order at most two and one of them is trivial. For the only case when it's not multiplicity free, by Proposition 2.2.3 (b), the homomorphism δ has a trivial image, hence the proof is also valid. \square

Proposition 3.2.2. *Let $A = \{c_1, c_3, \dots, c_{2g-1}\}$, $B = \{c_2, c_4, \dots, c_{2g}\}$ be the multi-curves on Σ_g as in Figure 1 with no multiplicities. We have*

$$\ker(\rho_{A,B}) = \langle \iota_g \rangle \cong \mathbb{Z}_2 .$$

Proof. It follows from the next lemmas. \square

Lemma 3.2.3. *Let T_{c_i} ($1 \leq i \leq 2g+1$) be the Dehn twists around simple closed curves as in Figure 1. Let $T_{A_g} := T_{c_1}T_{c_2} \dots T_{c_g}$, $T_{B_g} := T_{c_{g+1}}T_{c_{g+2}} \dots T_{c_{2g}}$ and $\iota_g = T_{c_{2g+1}}T_{c_{2g}} \dots T_{c_1}T_{c_1} \dots T_{c_{2g}}T_{c_{2g+1}}$ is a hyperelliptic involution shown in Figure 1, then we have the relation*

$$(4) \quad \begin{aligned} (T_{A_g}T_{B_g})^{2g+1} &= \iota_g , \\ (T_{A_g}^{-1}(T_{A_g}T_{B_g})^{g+1})^2 &= \iota_g . \end{aligned}$$

Proof. From direct computation only using braid group relations we have

$$(T_{A_g}T_{B_g}T_{c_{2g+1}})^{2g+2} = (T_{A_g}T_{B_g})^{2g+1}\iota_g .$$

Take a closed regular neighborhood of the union of curves c_i ($1 \leq i \leq 2g+1$), as the boundary of this neighborhood consists of two nullhomotopic simple closed curves, from the chain relation [12, Proposition 4.12], the left-hand side = 1 (it is not hard to get the same relation for right Dehn twists), hence we get first equality.

For the second relation, combined with the first one, it suffices to prove

$$(5) \quad T_{B_g}(T_{A_g}T_{B_g})^g = (T_{A_g}T_{B_g})^gT_{A_g} .$$

Now let $\sigma^n(T_{A_g}) = T_{c_{1+n}}T_{c_{2+n}} \dots T_{c_{g+n}}$, hence $\sigma^g(T_{A_g}) = T_{B_g}$. The following relation holds in \mathcal{B}_{2g+1} (since $T_{c_{i+1}}T_{A_g}T_{B_g} = T_{A_g}T_{B_g}T_{c_i}$), hence in $\text{Mod}(\Sigma_g)$

$$(6) \quad \sigma^m(T_{A_g})T_{A_g}T_{B_g} = T_{A_g}T_{B_g}\sigma^{m-1}(T_{A_g}) . \quad (m \leq g)$$

Now (5) follows from (6)

$$\begin{aligned}
(T_{A_g} T_{B_g})^g T_{A_g} &= (T_{A_g} T_{B_g})^{g-1} \sigma(T_{A_g})(T_{A_g} T_{B_g}) \\
&= \cdots = \sigma^g(T_{A_g})(T_{A_g} T_{B_g})^g \\
&= T_{B_g}(T_{A_g} T_{B_g})^g.
\end{aligned}$$

Hence the lemma is proved. \square

Lemma 3.2.4. *Same setting as before, let $T_{\tilde{A}_g} := T_{c_1} T_{c_3} \cdots T_{c_{2g-1}}$, $T_{\tilde{B}_g} := T_{c_2} T_{c_4} \cdots T_{c_{2g}}$, we have $T_{\tilde{A}_g} T_{\tilde{B}_g} = x_g^{-1} T_{A_g} T_{B_g} x_g$, where $x_g = T_{A_{g-1}} T_{B_{g-1}} x_{g-1}$, $x_1 = 1$.*

Proof. By moving the elements with a larger index to the left we can rewrite the product:

$$(7) \quad T_{\tilde{A}_g} T_{\tilde{B}_g} = T_{c_{2g-1}} T_{c_{2g}} T_{c_{2g-3}} T_{c_{2g-2}} \cdots T_{c_3} T_{c_4} T_{c_1} T_{c_2} .$$

Now we prove the lemma by induction. When $g = 1$, the statement is obvious, suppose it's true for $g = k$, then when $g = k + 1$ we have

$$\begin{aligned}
T_{\tilde{A}_{k+1}} T_{\tilde{B}_{k+1}} &= T_{c_{2k+1}} T_{c_{2k+2}} T_{\tilde{A}_k} T_{\tilde{B}_k} \\
&= T_{c_{2k+1}} T_{c_{2k+2}} (x_k^{-1} T_{A_k} T_{B_k} x_k) \\
&= x_k^{-1} T_{c_{2k+1}} T_{c_{2k+2}} T_{A_k} T_{B_k} x_k \quad (x_k \text{ commutes with } T_{c_l} \text{ for } l \geq k) \\
&= x_k^{-1} (T_{A_k} T_{B_k})^{-1} T_{A_k} T_{B_k} T_{c_{2k+1}} T_{c_{2k+2}} T_{A_k} T_{B_k} x_k \\
&= x_{k+1}^{-1} T_{A_{k+1}} T_{B_{k+1}} x_{k+1} .
\end{aligned}$$

\square

From Lemma 3.2.3 and 3.2.4, and the fact that ι_g commutes with all these Dehn twists, we have

$$(8) \quad (T_{\tilde{A}_g} T_{\tilde{B}_g})^{2g+1} = \iota_g .$$

Now from equation (8), $\iota_g \in \ker(\rho_{A,B})$, which has the order of at most 2 (Proposition 3.2.1). Hence the Proposition 3.2.2 is proved.

Theorem 3.2.5. *Let $T_J = \iota_g^g T_{\tilde{A}_g}^{-1} (T_{\tilde{A}_g} T_{\tilde{B}_g})^{g+1}$, we have an injective homomorphism $\rho : \tilde{\Gamma}_{2g+1} \rightarrow \text{SMod}(\Sigma_g) \subset \text{Mod}(\Sigma_g)$, by sending A_{2g+1} , B_{2g+1} , J to $T_{\tilde{A}_g}$, $T_{\tilde{B}_g}$, T_J respectively.*



FIGURE 3. A Heegaard splitting represented by $S \in \text{Mod}(\Sigma_g)$

Proof. The graph $\mathcal{G}(A, B)$ is of type A with $2g$ vertices, and it is not hard to orient curves so that their geometric and algebraic intersection numbers coincide as indicated in Figure 1 and Figure 2 (one may observe the difference coming from the parity of g). Therefore the map $\rho_{A, B}$ factors through $\text{SL}(2, \mathbb{R})$. Now from Theorem 2.1.2, 3.1.4, Proposition 3.2.2 and the fact that $\rho_{A, B}(\iota_g) = \rho_{A, B}((T_{\tilde{A}_g} T_{\tilde{B}_g})^{2g+1}) = -I$, we have

$$\tilde{\Gamma}_{2g+1} \cong \langle T_{\tilde{A}_g}, T_{\tilde{B}_g} \rangle \hookrightarrow \text{SMod}(\Sigma_g) .$$

□

Corollary 3.2.6. *We have $T_J^2 = \iota_g$ and $T_J = \iota_g^g (T_{\tilde{A}_g} T_{\tilde{B}_g})^g T_{\tilde{A}_g}$.*

Proof. From Theorem 3.2.5, it suffices to prove $J^2 = -I$, and $J = (-1)^g (A_{2g+1} B_{2g+1})^g A_{2g+1}$ in $\tilde{\Gamma}_{2g+1}$. The second relation follows from $((A_{2g+1} B_{2g+1})^g A_{2g+1})^2 = -I = (A_{2g+1} B_{2g+1})^{2g+1}$.

□

3.3. Geometric description of T_J . Now we give a geometric description of the element T_J . Consider the Heegaard splitting represented by Figure 3, and denote the

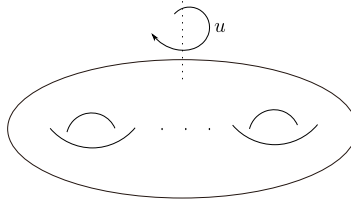


FIGURE 4. The element $u \in \text{Mod}(\Sigma_g)$

corresponding mapping class by S , S maps curves c_i to c_{i+1} for $1 \leq i \leq 2g$ and the image of c_0, c_{2g+1} under S is shown in the Figure 3. In fact, One can check directly $S = \prod_{i=1}^{2g+1} T_{c_i}$, which is a root of center in \mathcal{B}_{2g+2} . We denote the horizontal rotation in Figure 4 by u , It is clear $u \in \text{SMod}(\Sigma_g)$.

Lemma 3.3.1. *We have $T_J = \iota_g^g u S$ in $\text{Mod}(\Sigma_g)$.*

Proof. It suffices to show the actions of these two mapping classes agree on the simple closed curves c_i ($0 \leq i \leq 2g + 1$) with orientations. This can be done by directly working on the surface and comparing the two actions. While the action of $\iota_g^g u S$ is straightforward, the action of T_J can be more complicated. To address this, we utilize the flat structure defined in 3.2.2 and leverage the fact that the linear action of T_J is faithful (Theorem 3.2.5) and generally easier to describe with only a few exceptions.

Directly calculation shows $|c_i| = |c_{2g+1-i}|$ ($1 \leq i \leq 2g$), in fact we have [16]

$$\begin{aligned} v &= \left\{ \sin\left(\frac{1}{2g+1}\pi\right), \sin\left(\frac{3}{2g+1}\pi\right), \dots, \sin\left(\frac{2g-1}{2g+1}\pi\right) \right\}, \\ v' &= \left\{ \sin\left(\frac{2g-1}{2g+1}\pi\right), \sin\left(\frac{2g-3}{2g+1}\pi\right), \dots, \sin\left(\frac{1}{2g+1}\pi\right) \right\}. \end{aligned}$$

Hence the corresponding flat structure has a rotation-by- $\frac{\pi}{2}$ symmetry. By the result of Veech [38] discussed in the previous subsection, or see [28, Section 5] and Theorem 3.2.5, T_J is isotopic to the mapping class described in Figure 5 (here we give the proof for $g = 3$, but the proof works for any genus similarly). Then one can check geometrically how T_J moves the set of simple closed curves c_i for $0 \leq i \leq 2g + 1$ (Figure 1) and compare with the action of $\iota_g^g u S$ (It is clear how $\iota_g^g u S$ acts geometrically). If they agree on c_i for all $0 \leq i \leq 2g + 1$ (regard as the isotopy class), then $\iota_g^g u S T_J^{-1}$ will fix all c_i , hence, by Proposition 2.2.3 (b), commute with all the Dehn twists T_{c_i} generating $\text{Mod}(\Sigma_g)$. The result for $g \geq 3$ now follows from the fact that the center of $\text{Mod}(\Sigma_g)$ is trivial when $g \geq 3$. When $g = 1, 2$, the center is generated by the hyperelliptic involution ι_g , so it suffices to check their actions agree on some curve with orientations. One can see the action on c_0 and c_{2g+1} are the only non-obvious cases to check. For other curves, they are parallel to the edges of the cell decomposition, hence easy to see two mapping classes agree on c_i ($1 < i \leq 2g$) with orientations. We prove the case for c_0 and c_{2g+1} in Figure 5. We leave it to the reader to compare the curves in Figure 5 on the original surfaces. \square

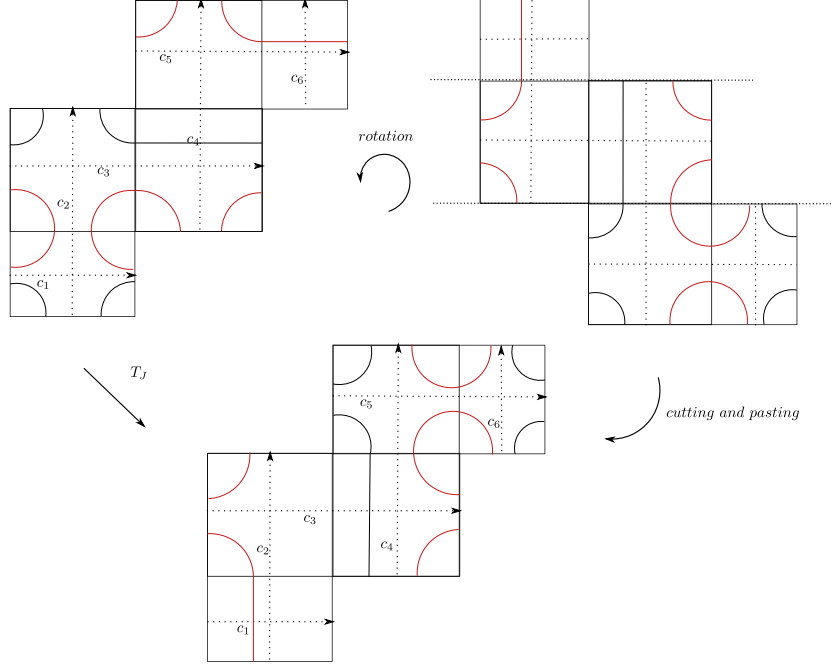


FIGURE 5. Action of T_J on the curve c_0 (red) and c_{2g+1} (black)

4. TOPOLOGICAL QUANTUM FIELD THEORY

4.1. **Notations.** The standard references are [5, 6, 33], Let integer $p \geq 3$, $r = p - 2$. We denote the color set by I_r . $I_r = \{0, 1, \dots, r\}$, when r is even, and $I_r = \{0, 2, \dots, r - 1\}$, when r is odd. Let A be a primitive $4p$ -th root of unity when r is even, and a primitive $2p$ -th root of unity when r is odd. For integer i , let $\Delta_i = (-1)^i [i + 1]$, where $[n] = \frac{A^{2n} - A^{-2n}}{A^2 - A^{-2}}$ is the quantum integer, and $\theta_i = (-1)^i A^{i(i-2)}$. We also let $\mathcal{P}_r^\pm = \sum_{i \in I_r} \theta_i^\pm \Delta_i^2$, $D_r = \sqrt{\sum_{i \in I_r} \Delta_i^2}$ and $\kappa_r = \frac{\mathcal{P}_r^+}{D_r} = \sqrt{\frac{\mathcal{P}_r^+}{\mathcal{P}_r^-}}$. H_g is the genus g handlebody.

Definition 4.1.1. Given a compact closed oriented three-manifold, the **skein space** $\mathcal{S}(M)$ is the vector space spanned by all the isotopy classes of framed links in M modulo Kaffuman bracket relations.

$$\begin{array}{c} \diagup \diagdown \\ \diagdown \diagup \end{array} = A \left| \begin{array}{c} | \\ | \end{array} \right. + A^{-1} \begin{array}{c} \cup \\ \cup \\ \cup \\ \cup \end{array} \quad \bigcirc = -A^2 - A^{-2}$$

In particular, $\mathcal{S}(S^3) = \mathbb{C}$.

Given a framed link and an integer r . One can color the curves using Jones-Wenzl idempotents f_i ($0 \leq i \leq r$) [18, 41]. Let $e_i \in \mathcal{S}(H_1)$ denote the single curve winding once around the longitude, colored with i -th Jones-Wenzl idempotent. Let $\Omega_r = \sum_{i \in I_r} \Delta_i e_i \in \mathcal{S}(H_1)$. We use $L(\Omega_r)$ to denote the link obtained by replacing each component of L by Ω_r , and $\langle L \rangle_r$ to denote the number we get by resolving the framed colored link L in S^3 .

4.2. Invariants. Let M_L be a three-dimensional manifold obtained by doing surgery along a framed link L in S^3 , we use $Z_r(M, L')$ to denote the Reshetikhin-Turaev (RT) invariant of M at level r with a framed colored link $L' \subset M$, we have $(\varsigma(L))$ is the signature of the linking matrix of L , and m is the number of components of L

$$(9) \quad Z_r(M_L, L') = (\mathcal{P}_r^-)^{\varsigma(L)} D^{-\varsigma(L)-m-1} \langle L(\Omega_r) \cup L' \rangle_r .$$

In particular, $Z_r(S^3) = D_r^{-1}$.

4.3. Vector space. The TQFT vector space of Σ_g is constructed as the quotient of $\mathcal{S}(H_g)$ by the left kernel of any sesquilinear form induced by gluing of handlebodies [6, Prop. 1.9]. It is a finite-dimensional vector space, and we will briefly recall the explicit basis constructed in [6], also see [23] for the pure skein construction.

Definition 4.3.1. *Given a trivalent vertex with edges colored by a, b, c from the set I_r . We say the vertex is **r -admissible** if the coloring satisfies:*

$$\begin{aligned} a + b + c &= 0 \pmod{2} , \\ |a - b| &\leq c \leq a + b , \\ a + b + c &\leq 2r . \end{aligned}$$

Definition 4.3.2. *An **r -admissible trivalent graph** is a labeled trivalent graph with all vertices r -admissible.*

Definition 4.3.3. *Let Σ_g be a (closed) surface bounding the handlebody H_g and Γ be a trivalent graph inside H_g to which H_g retracts. The **TQFT vector space at level r** is spanned by all the r -admissible trivalent graphs with Γ being the underlying graph, and all colors are from I_r . Figure 6 shows one possible underlying graph, admissibly coloring the graph produces one basis. We denote the basis vectors by u_σ , where σ is a function from the set of edges to I_r . We also denote the handlebody with a basis by H_g^σ , and we denote the TQFT vector space by $V_r(\Sigma_g)$. it corresponds to $SU(2)$ theory when r is even, and $SO(3)$ theory when r is odd.*

Moreover we let $d_r(g) := \dim(V_r(\Sigma_g))$, the dimension is given by the formula [6, Corollary 1.16]

$$(10) \quad d_r(g) = \begin{cases} \left(\frac{r+2}{2}\right)^{g-1} \sum_{j=1}^{r+1} \left(\sin \frac{2\pi j}{2r+4}\right)^{2-2g}, & \text{if } r \text{ is even;} \\ \left(\frac{r+2}{4}\right)^{g-1} \sum_{j=1}^{\frac{r+1}{2}} \left(\sin \frac{2\pi j}{r+2}\right)^{2-2g}, & \text{if } r \text{ is odd.} \end{cases}$$

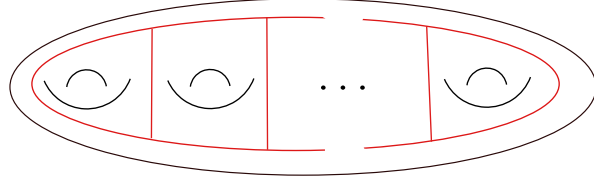


FIGURE 6. The underlying trivalent graph

One can relate different basis by doing F -moves locally showing in Figure 7, where $F_{i,j,n}^{k,l,m}$ is the $6j$ symbol $\begin{Bmatrix} k & l & m \\ i & j & n \end{Bmatrix}$, we also denote the tetrahedron coefficient by $\langle \begin{smallmatrix} * & * & * \\ * & * & * \end{smallmatrix} \rangle$, one can find explicit formulas in, for example, [27].

$$\begin{array}{c} i & & j \\ & \diagdown & / \\ & n & \\ & / & \diagdown \\ l & & k \end{array} = \sum_{m:(m,i,j) \text{ admissible}} F_{i,j,n}^{k,l,m} \begin{array}{c} i & & j \\ & \diagdown & / \\ & m & \\ & / & \diagdown \\ l & & k \end{array}$$

FIGURE 7. The F-move

For the more general setting, one can see, for example [37], where TQFT is constructed from modular categories, the coloring corresponds to the simple objects in the category and the edges are morphisms. In the $SU(2)$ and $SO(3)$ case, the corresponding modular categories here are the TLJ-category (Temperle-Lieb-Jones category) [37, 40], simple objects here are Jones-Wenzl projections [18, 41], which have nice diagrammatic descriptions [40].

4.4. Projective action of mapping class group. Let $f \in \text{Mod}(\Sigma_g)$, denote the corresponding mapping cylinder by $M_f = \Sigma_g \times [0, \frac{1}{2}] \cup_{(x, \frac{1}{2}) \sim (f(x), \frac{1}{2})} \Sigma_g \times [\frac{1}{2}, 1]$, fix a basis for $V_r(\Sigma_g)$ as in Definition 4.3.3, then we have a bilinear form $(\ , \)_f$ given by

$(u_\sigma, u_\mu)_f = Z_r(H_g^\sigma \cup_{id} M_f \cup_{id} \bar{H}_g^\mu)$. Where \bar{H}_g denotes H_g with opposite orientation (hence the framing of curves inside H_g will also be reversed). It is proven in [6] the bilinear form $(,)_f$ is nondegenerate (since the vector space is constructed by quotient out the kernel), and the form $(,)_r := (,)_{id}$ induced by identity mapping class is hermitian, and the basis defined in Definition 4.3.3 forms an orthogonal basis. Moreover we have [6, Theorem 4.11]:

$$(11) \quad (u_\sigma, u_\sigma)_r = D_r^{g-1} \frac{\prod_v \mathcal{T}_v}{\prod_e \Delta_{\sigma(e)}}$$

where $\mathcal{T}_v = \Delta_{i,j,k}$ given by evaluation of following diagram (i, j, k are colors of the edges intersecting at v).

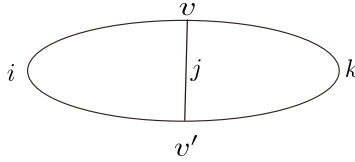


FIGURE 8. Theta diagram

In particular, let u_0 denote the basis vectors with zero coloring, one has

$$(12) \quad (u_0, u_0)_r = D_r^{g-1}.$$

Now the linear action can be computed by the bilinear form: $Z_r(M_f)_{\sigma,\mu} = \frac{(u_\sigma, u_\mu)_f}{(u_\mu, u_\mu)_r}$, and we have

$$(13) \quad (u_\sigma, u_\mu)_f = (Z_r(M_f)u_\sigma, u_\mu)_r.$$

The representation is projective since the signatures don't behave well with respect to the gluing see, for example [37, Section IV] and [26, Lemma 2.8].

When we pick special A , for example, $A = \pm i e^{\pm \frac{2\pi i}{4p}}$. The bilinear form $(,)_r$ gives an inner product on $V_p(\Sigma_g)$. After some normalizations, our $Z_r(M_f)$ will be unitary, hence it gives a unitary projective representation of $\text{Mod}(\Sigma_g)$. We will simply use $Z_r(f)$ to denote $Z_r(M_f)$.

It is in general very hard to compute directly, for example see [7] for the explicit formula for the set of Dehn twists generating the mapping class group, but for some special mapping classes it is easy to write down the matrix. When $f = T_\gamma$ is the right (left)

Dehn twist along a curve γ , then M_f can be presented by surgery on the curve $\gamma \times \{\frac{1}{2}\} \subset \Sigma_g \times I$, which is ∓ 1 framed relative to the surface $\Sigma_g \times \{\frac{1}{2}\}$ (denoted by γ^\mp). If γ bounds a disk in H_g , for example curves $\{c_0, c_1, c_3, \dots, c_{2g+1}\}$, it is easy to resolve the diagrams and compute the invariant using Kirby calculus. One has

$$(14) \quad Z_r(T_\gamma)u_\sigma = \theta_{\sigma(e_\gamma)}u_\sigma.$$

Where e_γ is the edge transverse to the disk bounded by γ (if such edge exists in the underlying graph for the basis).

When f corresponds to a Heegaard splitting of the S^3 , from the above discussion and the Formula (9), We have

$$Z_r(S^3, L) = Z_r(S^3) \langle L \rangle_r = D^{-1} \langle L \rangle_r .$$

Hence the entry of the $Z_r(M_f)$ can be computed by evaluating some tangle diagrams in S^3 , and this is how we compute $Z_r(T_J)$. The diagram presentation for $Z_r(T_J)$ can be obtained easily from Lemma 3.3.1, see Figure 11 for the case when $g = 2$.

There are some useful skein identities, for example in [20, 27], we list some we need here.

FIGURE 9. Partition of identity

FIGURE 10. Two skein identities

Now we will briefly describe two projective actions defined in [33], also see [26]. One is geometric, the other is skein theoretic, we denote them by ϕ_1 and ϕ_2 respectively. They give the same projective representation but slightly different central extensions [26], also see [15].

Fix a Heegaard splitting of S^3 corresponding to some mapping class, for example the mapping class T_J as defined in Theorem 3.2.5 (also see Lemma 3.3.1), we have $S^3 = H_g \cup_{T_J} \bar{H}_g = H_g \cup_{\Sigma_g \times \{0\}} (\Sigma_g \times I) \cup_{\Sigma_g \times \{1\}} \bar{H}'_g$, then $V_r(\Sigma_g)$ can be viewed as the quotient of $\mathfrak{S}(H_g)$ by the kernel of the form $(\ , \)_{T_J}$. There are natural left and right actions of $\mathfrak{S}(\Sigma_g \times I)$ on $V_r(\Sigma_g)$ by pushing the curves in $\Sigma_g \times I$ into H_g and H'_g , and $\mathfrak{S}(\Sigma_g \times I)$ is itself an algebra. Moreover it is a $*$ -algebra, where the $*$ structure is induced by the map $id \times (-1)$ on $\Sigma \times I$. In particular it reverses framings relative to the surface, we use $\bar{\gamma}$ to denote the γ under the $*$ operation. We also denote the left action by $\text{Add} : \mathfrak{S}(\Sigma_g \times I) \rightarrow \text{End}(V_r(\Sigma_g))$, one has

$$(15) \quad (\text{Add}(\gamma)u_\sigma, u_\mu)_r = (u_\sigma, \text{Add}(\bar{\gamma})u_\mu)_r.$$

Now since $\text{Mod}(\Sigma_g)$ acts naturally on $\Sigma_g \times I$, it acts on $\mathfrak{S}(\Sigma_g \times I)$. It is proved in [33] that Add is surjective, and moreover the kernel of Add is preserved by the action of $\text{Mod}(\Sigma_g)$. Therefore $\text{Mod}(\Sigma_g)$ induces automorphisms of $\text{End}(V_r(\Sigma_g))$, it is inner since $V_r(\Sigma_g)$ is finite dimensional. As a result, for any $f \in \text{Mod}(\Sigma_g)$, there exists $\Phi(f) \in \text{End}(V_r(\Sigma_g))$ such that for any $\gamma \in \mathfrak{S}(\Sigma_g \times I)$ we have

$$(16) \quad \text{Add}(f(\gamma)) = \Phi(f) \text{Add}(\gamma)(\Phi(f))^{-1}.$$

Note $\Phi(f)$ is only well defined up to a constant, hence gives a projective representation. It is not hard to see $Z_r(T_J)$ satisfies (16) for any $\gamma \in \mathfrak{S}(\Sigma_g \times I)$, indeed one observe

$$(\text{Add}(\gamma)u_\sigma, u_\mu)_{T_J} = (u_\sigma, \text{Add}(\overline{T_J(\gamma)})u_\mu)_{T_J},$$

hence by (13), we have for any $u_\sigma, u_\mu \in V_r(\Sigma_g)$,

$$(17) \quad \begin{aligned} (Z_r(T_J) \text{Add}(\gamma)u_\sigma, u_\mu)_r &= (Z_r(T_J)u_\sigma, \text{Add}(\overline{T_J(\gamma)})u_\mu)_r, \\ &= (\text{Add}(T_J(\gamma))Z_r(T_J)u_\sigma, u_\mu)_r. \end{aligned}$$

Now we will describe two actions.

Geometric action is defined on mapping classes which can be extended in H_g or H'_g , we denote such mapping classes by K, K' respectively. Such mapping classes directly act on the diagrams inside handlebodies, we denote the action by \tilde{f} . If $f \in K$, one define $\phi_1(u_\sigma) = \tilde{f}(u_\sigma)$. If $f \in K'$, define $\phi_1(f)$ by

$$(18) \quad (\phi_1(f)u_\sigma, u_\mu)_{T_J} = (u_\sigma, \tilde{f}^{-1}(u_\mu))_{T_J}.$$

One can check the action ϕ_1 satisfies (16) [33], and since K, K' generates $\text{Mod}(\Sigma_g)$, as a projective representation we have $\phi_1 = \Phi$, and in particular, we have

$$(19) \quad Z_r(T_J) = c_1 \phi_1(T_J)$$

for some nonzero constant c_1 (which depends on the choice of $K \cup K'$ word representing T_J). Now for Dehn twists along curves $\{c_0, c_1, c_3, \dots, c_{2g+1}\}$ which are in K . They are diagonal matrices given by

$$(20) \quad \phi_1(T_\gamma)u_\sigma = \theta_{\sigma(e_\gamma)}u_\sigma.$$

For Dehn twists along curves $\{c_2, \dots, c_{2g}\}$ which are in K' , see Figure 3 and Lemma 3.3.1. From (18), (20) and similar argument as in (17), we have for $1 \leq i \leq g$

$$(21) \quad \phi_1(T_{c_{2i}}) = Z_r(T_J)\phi_1(T_{c_{2g+1-2i}})Z_r(T_J)^{-1}.$$

Skein theoretic action is defined on the set of all the Dehn twists, denoted by \mathcal{D} , it is motivated by the surgery presentation of mapping cylinder corresponding to the Dehn twists as discussed above. Similarly, let T_γ be the right (left) Dehn twist along a curve γ , then the action $\phi_2(T_\gamma)$ is given by first cabling the curve $\gamma^\mp \subset \Sigma_g \times I$ by the skein element $\kappa_r^\pm \frac{\Omega_r}{D}$ in $\mathcal{S}(H_1)$, and then pushing it back in the handlebody H_g , namely $\phi_2(T_\gamma) = \text{Add}(\gamma^\mp(\kappa_r^\pm \frac{\Omega_r}{D}))$. Now if γ bounds a disk in H_g , for example curves $\{c_0, c_1, c_3, \dots, c_{2g+1}\}$, we have similarly

$$(22) \quad \phi_2(T_\gamma)u_\sigma = \theta_{\sigma(e_\gamma)}u_\sigma,$$

If γ does not bound a disk, for example curves $\{c_2, c_4, \dots, c_{2g}\}$, one can make use of the Proposition 2.2.3 (a), so that γ can be map to the curves that bound a disk. For example the mapping class T_J , we have $T_J(c_i) = c_{2g+1-i}$ for $1 \leq i \leq 2g$. Hence by (16), we have for $1 \leq i \leq g$,

$$(23) \quad \phi_2(T_{c_{2i}}) = Z_r(T_J)\phi_2(T_{c_{2g+1-2i}})Z_r(T_J)^{-1} = \phi_1(T_J)\phi_2(T_{c_{2g+1-2i}})\phi_1(T_J)^{-1}.$$

Compare equation (20) and (22), also from (23), we have $\phi_1 = \phi_2$ as projective representations. In particular

$$(24) \quad Z_r(T_J) = c_2\phi_2(T_J).$$

for some nonzero constant c_2 (which depends on the choice of \mathcal{D} word representing T_J).

It is not hard to see ϕ_1 and ϕ_2 agree on the word in $\mathcal{D} \cap (K \cup K')$ from (20)-(23) and they are homomorphisms when restricted to $K(\cap \mathcal{D})$ or $K'(\cap \mathcal{D})$. Moreover they are unitary when the hermitian form is positive definite, see [33, 26] for more details.

Remark 4.4.1. The equality in (23) allows one to compare the projective factors between two actions, see [26]. Thanks to (19) (24), we can extend their result to the mapping class T_J , so that c_1, c_2 can also be determined similarly as in the proof of [26, Lem. 2.8].

Lemma 4.4.2. *We have $Z_r(T_J)^2 = \phi_1(\iota_g)$.*

Proof. Let c be the $(1, 1)$ -entry of the matrix $(Z_r(T_J))^2$. Since $T_J^2 = \iota_g$, and

$$(\phi_1(\iota_g)u_0, u_0)_r = (u_0, u_0)_r ,$$

it suffices to prove $c = 1$. We have

$$c = \sum_{\sigma} \frac{(u_0, u_{\sigma})_{T_J} (u_{\sigma}, u_0)_{T_J}}{(u_{\sigma}, u_{\sigma})_r (u_0, u_0)_r}.$$

From Lemma 3.3.1, and the standard calculations using second identity in Figure 10, we have $(u_{\sigma}, u_0)_{T_J} = (u_0, u_{\sigma})_{T_J} = D_r^{-1} \langle u_{\sigma} \rangle_r$. It is nonzero if and only if $\phi_1(\iota_g)u_{\sigma} = u_{\sigma}$. Therefore by (11), we have

$$\begin{aligned} c &= D_r^{-2} \sum_{\sigma: \phi_1(\iota_g)u_{\sigma}=u_{\sigma}} \frac{\langle u_{\sigma} \rangle_r^2}{(u_{\sigma}, u_{\sigma})_r (u_0, u_0)_r} , \\ &= D_r^{-2g} \sum_{\sigma: \phi_1(\iota_g)u_{\sigma}=u_{\sigma}} \prod_{e \in E'} \Delta_{\sigma(e)} , \end{aligned}$$

where E' is the set of edges (in Figure 6) that invariant under the action of ι_g . Now consider g unknots placed next to each other and all colored with Ω_r , there are two ways to evaluate it. Direct evaluation gives D_r^{2g} , the other way is to apply the partition of identity (Figure 9) $g - 1$ times, one gets a linear combination of u_{σ} . Resolving it using the second identity in Figure 10 as before, one gets number $\prod_{e \in E'} \Delta_{\sigma(e)}$. Therefore $c = 1$. \square

Lemma 4.4.3. *Let w_1 be a K word, w_2 be a \mathcal{D} word, and $w_2 w_1$ ($w_1 w_2$ if w_1 is a K' word) is a word representing the mapping class T_J , we have*

$$(25) \quad \phi_2(w_2)\phi_1(w_1) = \kappa_r^{\zeta(w_2)+e(w_2)} Z_r(T_J) ,$$

where $\zeta(w) = \varsigma(L_w)$ is the signature of link L_w defined in [26, Sec. 2.3], and $e(w_2)$ is the exponent sum of the word w_2 .

Proof. We have

$$\begin{aligned} (\phi_2(w_2)\phi_1(w_1)u_0, u_0)_{T_J} &= (\phi_2(w_2)\tilde{w}_1(u_0), u_0)_{T_J}, \\ &= (\phi_2(w_2)u_0, u_0)_{T_J}, \\ &= \kappa_r^{\zeta(w_2)+e(w_2)} Z_r(M_{L_{w_2}}). \end{aligned}$$

Now since the closed manifold $M_{L_{w_2}}$ is homeomorphic to the manifold

$$\begin{aligned} H_g \cup_{id} M_{T_J w_1^{-1}} \cup_{id} \bar{H}'_g &\simeq H_g \cup_{id} M_{T_J w_1^{-1}} \cup_{id} M_{T_J} \cup_{id} \bar{H}_g , \\ &\simeq H_g \cup_{id} M_{\iota_g} \cup_{id} \bar{H}_g , & (w_1^{-1} \in K, \text{ and } T_J^2 = \iota_g) \\ &\simeq H_g \cup_{id} \Sigma_g \times I \cup_{id} \bar{H}_g . & (\iota_g \in K \cap K') \end{aligned}$$

We have $Z_r(M_{L_{w_2}}) = (u_0, u_0)_r$, and the lemma follows from (13) and Lemma 4.4.2

$$(Z_r(T_J)u_0, u_0)_{T_J} = ((Z_r(T_J))^2 u_0, u_0)_r = (u_0, u_0)_r .$$

□

Proposition 4.4.4. *Let w be the \mathcal{D} word $(T_{\tilde{A}_g} T_{\tilde{B}_g})^g T_{\tilde{A}_g}$, we have*

$$(26) \quad (\phi_1(T_{\tilde{A}_g}) Z_r(T_J))^{2g+1} = \kappa_r^{\tilde{\zeta}(w)+g(2g+1)} \phi_1(\iota_g).$$

Proof. From Lemma 4.4.2, we have $Z_r(T_J) = \phi_1(\iota_g)(Z_r(T_J))^{-1}$. Hence from (21) or (23), we have $Z_r(T_J)\phi_i(T_{\tilde{A}_g})Z_r(T_J) = \phi_i(T_{\tilde{B}_g})\phi_1(\iota_g)$ for $i = 1, 2$ (ϕ_1, ϕ_2 agrees on those Dehn twists). Now since all the mapping classes related are in $\text{SMod}(\Sigma_g)$, they commute with ι_g . Moreover since $\iota_g \in K \cap K'$, by similar but simpler argument as in Lemma 4.4.3, we have in particular $\phi_1(\iota_g)$ commutes with $\phi_i(T_{\tilde{A}_g})$ and $\phi_i(T_{\tilde{B}_g})$ for $i = 1, 2$. Therefore we have

$$(\phi_1(T_{\tilde{A}_g}) Z_r(T_J))^{2g+1} = \phi_1(\iota_g^g) \phi_2(w) Z_r(T_J).$$

Since $T_J = \iota_g^g (T_{\tilde{A}_g} T_{\tilde{B}_g})^g T_{\tilde{A}_g}$ (Corollary 3.2.6), the second equality follows from Lemma 4.4.2 and 4.4.3.

□

Now we are ready for the main theorem.

Theorem 4.4.5. *We have projective (unitary) representations h_r of $\tilde{\Gamma}_{2g+1}$ from the TQFT vector spaces $V_r(\Sigma_g)$, and when $g \leq 2$ the representations factor through Γ_{2g+1} . In particular. When $g = 1$, $h_r(A_1), h_r(J)$ gives the modular data of TLJ modular categories, when $g = 2$, we have $\mathcal{J}_r := h_r(J)$ and a diagonal matrix $\mathcal{T}_r := h_r(A_3)$, satisfying the relations:*

$$(27) \quad \begin{aligned} \mathcal{J}_r^2 &= I , \\ (\mathcal{T}_r \mathcal{J}_r)^5 &= \left(\frac{\mathcal{P}_r^+}{\mathcal{P}_r^-} \right)^2 I . \end{aligned}$$

Proof. Let $h_r(A_{2g+1}) := \phi_1(T_{\tilde{A}_g})$ and $h_r(J) := Z_r(T_J)$. From Lemma 4.4.2, Proposition 4.4.4 and Theorem 3.2.5, it gives a projective representation of $\tilde{\Gamma}_{2g+1}$. One can get a unitary representation by specializing A to some appropriate root of unity, for example, $A = \pm i e^{\pm \frac{2\pi i}{4p}}$. Normalizing the basis using (11), under normalized basis, ϕ_1 and ϕ_2 are unitary ([33]). In particular, up to a scalar, $Z_r(T_J)$ is unitary. Since its first row and column are all real numbers, the same computation as in the proof of Lemma 4.4.2 shows that $Z_r(T_J)$ is indeed unitary. For $g = 1, 2$, it's straight forward to see $\phi_1(\iota_g) = I$. The special cases in the theorem now follow from the computation of the signatures, when $g = 1$, $\zeta(w) = -2$, and when $g = 2$, $\zeta(w) = -6$. \square

Remark 4.4.6. Theorem 4.4.5 and Proposition 4.4.4 imply h_r can be lifted to a linear representation \tilde{h}_r by multiplying a root of unity \varkappa in \mathcal{T}_r , provided $\varkappa^{2g+1} = \kappa_r^{\zeta(w)+g(2g+1)}$.

In the rest of this section, we will focus on the case where $g = 2$, and we will give concrete calculations. We denote the basis in $V_r(\Sigma_2)$ by u_{ijk} , which means the graph in Figure 6 is colored by i, j, k from left to right, and we give them the dictionary order. Let $\tilde{\mathcal{J}}_{i_1 j_1 k_1, i_2 j_2 k_2} := (u_{i_1 j_1 k_1}, u_{i_2 j_2 k_2})_{T_J}$, the matrix $\tilde{\mathcal{J}}$ can be computed from evaluating the following diagrams.

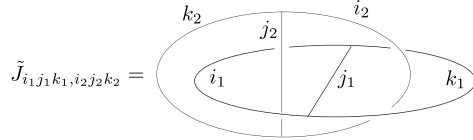


FIGURE 11. The diagram presentation for $Z_r(T_J)$

Therefore it is easy to see $\tilde{\mathcal{J}}$ is a symmetric real matrix. And we have

$$(28) \quad \mathcal{J}_{i_1 j_1 k_1, i_2 j_2 k_2} = \frac{\Delta_{i_2} \Delta_{j_2} \Delta_{k_2}}{D^2 \Delta_{i_2 j_2 k_2}^2} \tilde{\mathcal{J}}_{i_1 j_1 k_1, i_2 j_2 k_2} ,$$

$$\mathcal{T}_r u_{ijk} = \theta_i \theta_j u_{i,j,k} .$$

When the form $(,)$ is positive definite one can normalize the basis, we have a unitary matrix

$$(29) \quad \mathcal{J}_{i_1 j_1 k_1, i_2 j_2 k_2} = \frac{\sqrt{\Delta_{i_1} \Delta_{j_1} \Delta_{k_1} \Delta_{i_2} \Delta_{j_2} \Delta_{k_2}}}{D^2 \Delta_{i_1, j_1, k_1} \Delta_{i_2, j_2, k_2}} \tilde{\mathcal{J}}_{i_1 j_1 k_1, i_2 j_2 k_2} .$$

\mathcal{T}_r is a diagonal matrix and the entries are all root of unities, hence always unitary.

Now we give a formula to evaluate entries of \tilde{J}

Proposition 4.4.7. *We have*

$$(30) \quad \tilde{J}_{i_1 j_1 k_1, i_2 j_2 k_2} = \sum_{l=0}^{r-2} \Delta_l^{-1} a_l^{j_1, i_2} \bar{a}_l^{k_2, i_1} \left\langle \begin{matrix} l & i_2 & i_2 \\ j_2 & k_2 & k_2 \end{matrix} \right\rangle \left\langle \begin{matrix} l & j_1 & j_1 \\ k_1 & i_1 & i_1 \end{matrix} \right\rangle.$$

where $a_k^{i,j}$ is the coefficient of the following recoupling formula:

and

$$(31) \quad a_l^{i,j} = \sum_{k:(i,j,k) \text{ } r\text{-admissible}} \Delta_k \theta_i \theta_j \theta_k^{-1} \Delta_{i,j,k}^{-1} \left\{ \begin{matrix} i & j & l \\ j & i & k \end{matrix} \right\}.$$

Proof. Equation (31) follows from applying the identity on the left of Figure 10 and a F-move. Now one can resolve two double crossings in the diagram presentation of \tilde{J} , and apply the identity on the right of Figure 10. The remaining diagram is two tetrahedrons connected along an edge, straightforward computations give us the Formula (30). \square

Remark 4.4.8. Similar diagrams (as in figure 11) also appear in [24] as certain dualities of the Fourier transform.

Now we give the calculation result for Ising theory $r = 2, A = ie^{\frac{\pi}{8}i}$ and Fibonacci theory $r = 3, A = ie^{\frac{\pi}{10}i}$, which are done easily by hand and verified by using Maple software, see Appendix A:

$$\mathcal{J}_2 = \begin{pmatrix} \frac{1}{4} & \frac{\sqrt{2}}{4} & \frac{1}{4} & \frac{\sqrt{2}}{4} & \frac{\sqrt{2}}{4} & \frac{\sqrt{2}}{4} & \frac{\sqrt{2}}{4} & \frac{1}{4} & \frac{\sqrt{2}}{4} & \frac{1}{4} \\ \frac{\sqrt{2}}{4} & \frac{1}{2} & \frac{\sqrt{2}}{4} & 0 & 0 & 0 & 0 & -\frac{\sqrt{2}}{4} & -\frac{1}{2} & -\frac{\sqrt{2}}{4} \\ \frac{1}{4} & \frac{\sqrt{2}}{4} & \frac{1}{4} & -\frac{\sqrt{2}}{4} & -\frac{\sqrt{2}}{4} & -\frac{\sqrt{2}}{4} & -\frac{\sqrt{2}}{4} & \frac{1}{4} & \frac{\sqrt{2}}{4} & \frac{1}{4} \\ \frac{\sqrt{2}}{4} & 0 & -\frac{\sqrt{2}}{4} & 0 & \frac{1}{2} & -\frac{1}{2} & 0 & -\frac{\sqrt{2}}{4} & 0 & \frac{\sqrt{2}}{4} \\ \frac{\sqrt{2}}{4} & 0 & -\frac{\sqrt{2}}{4} & \frac{1}{2} & 0 & 0 & -\frac{1}{2} & \frac{\sqrt{2}}{4} & 0 & -\frac{\sqrt{2}}{4} \\ \frac{\sqrt{2}}{4} & 0 & -\frac{\sqrt{2}}{4} & -\frac{1}{2} & 0 & 0 & \frac{1}{2} & \frac{\sqrt{2}}{4} & 0 & -\frac{\sqrt{2}}{4} \\ \frac{\sqrt{2}}{4} & 0 & -\frac{\sqrt{2}}{4} & 0 & -\frac{1}{2} & \frac{1}{2} & 0 & -\frac{\sqrt{2}}{4} & 0 & \frac{\sqrt{2}}{4} \\ \frac{1}{4} & -\frac{\sqrt{2}}{4} & \frac{1}{4} & -\frac{\sqrt{2}}{4} & \frac{\sqrt{2}}{4} & \frac{\sqrt{2}}{4} & -\frac{\sqrt{2}}{4} & \frac{1}{4} & -\frac{\sqrt{2}}{4} & \frac{1}{4} \\ \frac{\sqrt{2}}{4} & -\frac{1}{2} & \frac{\sqrt{2}}{4} & 0 & 0 & 0 & 0 & -\frac{\sqrt{2}}{4} & \frac{1}{2} & -\frac{\sqrt{2}}{4} \\ \frac{1}{4} & -\frac{\sqrt{2}}{4} & \frac{1}{4} & \frac{\sqrt{2}}{4} & -\frac{\sqrt{2}}{4} & -\frac{\sqrt{2}}{4} & \frac{\sqrt{2}}{4} & \frac{1}{4} & -\frac{\sqrt{2}}{4} & \frac{1}{4} \end{pmatrix}$$

$$\mathcal{T}_2 = \begin{pmatrix} 1 & 0 & 0 & 0 & 0 & 0 & 0 & 0 & 0 & 0 \\ 0 & e^{\frac{7\pi i}{8}} & 0 & 0 & 0 & 0 & 0 & 0 & 0 & 0 \\ 0 & 0 & -1 & 0 & 0 & 0 & 0 & 0 & 0 & 0 \\ 0 & 0 & 0 & e^{\frac{7\pi i}{8}} & 0 & 0 & 0 & 0 & 0 & 0 \\ 0 & 0 & 0 & 0 & -e^{\frac{3\pi i}{4}} & 0 & 0 & 0 & 0 & 0 \\ 0 & 0 & 0 & 0 & 0 & -e^{\frac{3\pi i}{4}} & 0 & 0 & 0 & 0 \\ 0 & 0 & 0 & 0 & 0 & 0 & -e^{\frac{7\pi i}{8}} & 0 & 0 & 0 \\ 0 & 0 & 0 & 0 & 0 & 0 & 0 & -1 & 0 & 0 \\ 0 & 0 & 0 & 0 & 0 & 0 & 0 & 0 & -e^{\frac{7\pi i}{8}} & 0 \\ 0 & 0 & 0 & 0 & 0 & 0 & 0 & 0 & 0 & 1 \end{pmatrix}$$

$$\mathcal{J}_3 = \begin{pmatrix} \frac{5-\sqrt{5}}{10} & \frac{\sqrt{5}}{5} & \frac{\sqrt{5}}{5} & \frac{\sqrt{5}}{5} & \frac{\sqrt{10(1+\sqrt{5})}}{10} \\ \frac{\sqrt{5}}{5} & \frac{5+\sqrt{5}}{10} & -\frac{5-\sqrt{5}}{10} & -\frac{5-\sqrt{5}}{10} & -\frac{\sqrt{10(\sqrt{5}-1)}}{10} \\ \frac{\sqrt{5}}{5} & -\frac{5-\sqrt{5}}{10} & -\frac{5-\sqrt{5}}{10} & \frac{5+\sqrt{5}}{10} & -\frac{\sqrt{10(\sqrt{5}-1)}}{10} \\ \frac{\sqrt{5}}{5} & -\frac{5-\sqrt{5}}{10} & \frac{5+\sqrt{5}}{10} & -\frac{5-\sqrt{5}}{10} & -\frac{\sqrt{10(\sqrt{5}-1)}}{10} \\ \frac{\sqrt{10(1+\sqrt{5})}}{10} & -\frac{\sqrt{10(\sqrt{5}-1)}}{10} & -\frac{\sqrt{10(\sqrt{5}-1)}}{10} & -\frac{\sqrt{10(\sqrt{5}-1)}}{10} & \frac{5-\sqrt{5}}{5} \end{pmatrix}$$

$$T_3 = \begin{pmatrix} 1 & 0 & 0 & 0 & 0 \\ 0 & e^{\frac{4}{5}\pi i} & 0 & 0 & 0 \\ 0 & 0 & e^{\frac{4}{5}\pi i} & 0 & 0 \\ 0 & 0 & 0 & e^{-\frac{2}{5}\pi i} & 0 \\ 0 & 0 & 0 & 0 & e^{-\frac{2}{5}\pi i} \end{pmatrix}$$

In particular, we have

Proposition 4.4.9. *The group $\tilde{h}_3(\Gamma_5)$ is infinite.*

Proof. Since the projective factor is a root of unity, it suffices to work with h_r . We compute the element $h_3(A_5B_5^{-1}) = \mathcal{J}_3\mathcal{T}_3\mathcal{J}_3\mathcal{T}_3^{-1}$. It has an eigenvalue $\frac{1}{4}(3 - \sqrt{5} + i\sqrt{2(1 + 3\sqrt{5})})$, which is not a root of unity, since its minimal polynomial, $1 - 3x + 3x^2 - 3x^3 + x^4$, is not cyclotomic. \square

Moreover since all the entries of matrices under unnormalized basis are in a cyclotomic field $\mathbb{Q}(A)$ (only even powers of D_r and κ_r appear when $g = 2$), the Galois group $\text{Gal}(\mathbb{Q}(A); \mathbb{Q})$ naturally acts on the representations. In particular, it preserves the property that the image is finite or not. Now let $A = e^{\frac{\pi i}{r}}$ for odd r . By computing the trace of the image of the Pseudo-Anosov mapping class $\rho(A_{2g+1}B_{2g+1}^{-1})$, we have

$$\text{Tr}(\mathcal{J}_r\mathcal{T}_r\mathcal{J}_r\mathcal{T}_r^{-1}) = \sum_{u_{i_1j_1k_1}, u_{i_2j_2k_2}} \theta_{i_1}\theta_{j_1}\theta_{i_2}^{-1}\theta_{j_2}^{-1}\mathcal{J}_{i_1j_1k_1, i_2j_2k_2}\mathcal{J}_{i_2j_2k_2, i_1j_1k_1},$$

and

Proposition 4.4.10. *The group $\tilde{h}_r(\Gamma_5)$ is also infinite for $r = 7, 9, 11, 13$.*

Proof. It suffices to check $\text{Tr}(\mathcal{J}_r\mathcal{T}_r\mathcal{J}_r\mathcal{T}_r^{-1}) \geq d_r(2)$. Using Maple software we have the following numerical results.

r	3	5	7	9	11	13
$d_r(g)$	5	14	30	55	91	140
Tr	4.24	10.54	32.16	102.92	332.49	1084.12

We have $\text{Tr}(\mathcal{J}_r\mathcal{T}_r\mathcal{J}_r\mathcal{T}_r^{-1}) \geq d_r(2)$ when $r = 7, 9, 11, 13$, which complete the proof. \square

5. SPIN STRUCTURE AND REDUCIBILITY

The $\mathbb{Z}/2\mathbb{Z}$ spin structure on a closed surface Σ_g of genus g is cohomology class $\varphi \in H^1(UT\Sigma_g, \mathbb{Z}/2\mathbb{Z})$ which evaluates to one on the oriented fiber of the unit tangent bundle $UT\Sigma_g \rightarrow \Sigma_g$. In [17], Johnson built a one-to-one correspondence between the set of $\mathbb{Z}/2\mathbb{Z}$ spin structures on a Riemann surface Σ_g with the set of $\mathbb{Z}/2\mathbb{Z}$ valued quadratic forms on $H_1(\Sigma_g, \mathbb{Z}/2\mathbb{Z})$ with associated intersection form on Σ_g (i.e. $q(a + b) = q(a) + q(b) + a \cdot b$). Moreover the bijection intertwines the action of $\text{Mod}(\Sigma_g)$ (induced by the obvious action of $Sp(2g, \mathbb{Z}/2\mathbb{Z})$), and there are two orbits of the action depending on

the parity of the spin structures, namely, the Arf invariant, which is an element in $\mathbb{Z}/2\mathbb{Z}$ defined by

$$\text{Arf}(q) = \sum_{i=1}^g q(x_i)q(y_i) ,$$

which is independent of the choice of symplectic basis x_i, y_i for $H_1(\Sigma_g, \mathbb{Z}/2\mathbb{Z})$. The TQFT vector space $V_r(\Sigma_g)$, for $4 \mid p (= r + 2)$, can be decomposed with respect to the spin structures on Σ_g . Recall for the action of Dehn twist along a curve on the $V_p(\Sigma_g)$ can be described by twisting the curve (make it -1 -framed) in $\Sigma_g \times \{\frac{1}{2}\} \subset \Sigma_g \times I$, attach a skein element and then push it back in the handlebody. Now we consider the curves in $H_1(\Sigma_g, \mathbb{Z}/2\mathbb{Z})$ as the curves in $\Sigma_g \times \{\frac{1}{2}\} \subset \Sigma_g \times I$, attached with the label r , then there is a natural action by pushing it in the handlebody (Add). It is straightforward to show the action is in fact unitary [6, Prop 7.5]. Moreover the product induced by the algebra structure of $\mathcal{S}(\Sigma_g \times I)$ gives the set of curves a structure of finite Heisenberg group (with the associated intersection form on Σ_g) $\mathbb{Z}/2\mathbb{Z} \times H_1(\Sigma_g, \mathbb{Z}/2\mathbb{Z})$ [6]. Which is abelian and the characters are giving by $\mathbb{Z}/2\mathbb{Z}$ valued quadratic forms on $H_1(\Sigma_g, \mathbb{Z}/2\mathbb{Z})$. Therefore one gets the decomposition

$$V_r(\Sigma_g) = \bigoplus_q V_r(\Sigma_g, q),$$

where each $V_r(\Sigma_g, q)$ is the direct sum of the one-dimensional representation associate with the quadratic form q . Two orbits (parity) give two invariant subspaces V_r^0, V_r^1 under $\text{Mod}(\Sigma_g)$ action and the associate vector spaces for spin structures of the same parity have the same dimensions, which are denoted by $d_r^0(g), d_r^1(g)$ respectively. We have $\dim(V^\epsilon) = 2^{g-1}(2^g + (-1)^\epsilon)d_g^\epsilon$, for $\epsilon \in \{0, 1\}$. The formula for $d_r^\epsilon(g)$ is given by [6, Thm 7.16]

$$(32) \quad d_r^\epsilon(g) = 2^{-2g}(d_r(g) + (\frac{r+2}{2})^{g-1}((-1)^\epsilon 2^g - 1)) .$$

Theorem 5.1. *when $g \geq 2$, $r = 4l + 2$ ($l \geq 1$), the representation \tilde{h}_r is reducible and has at least three irreducible summands.*

Proof. We choose oriented curves $\{\alpha_i, \beta_i\}_{1 \leq i \leq g}$ representing the standard symplectic basis. The spin structure associated with the flat structure can be described by a quadratic form that assigns number $(\text{ind}_\gamma + 1) \pmod{2}$ to γ (for $\gamma \in \{\alpha_i, \beta_i\}_{1 \leq i \leq g}$) [21, Section 3], where ind_γ is the index of the curve γ . For example in Figure 5, we have $\text{ind}_{c_i} = 0$ for $1 \leq i \leq 6$, $\text{ind}_{c_0} = 1$ and $\text{ind}_{c_7} = 2$. Hence it is not hard to calculate its parity, which is equal to $\sum_{i=1}^g (0 + 1)(i - 1 + 1) = \frac{(g+1)g}{2} \pmod{2}$. Now the group

generated by T_A, T_B fixes the flat structure, hence it fixes the associated spin structure, denoted by q_ω . We have following decomposition

$$V_r(\Sigma_g) = V_r(\Sigma_g, q_\omega) \oplus (V_r^0 \cap V_r^\perp(\Sigma_g, q_\omega)) \oplus (V_r^1 \cap V_r^\perp(\Sigma_g, q_\omega))$$

from the dimension counting of the TQFT vector spaces associated with spin structures (32), when $g \geq 2$, $l \geq 1$, dimensions for three summands are all nonzero. □

APPENDIX A. MAPLE CODE

Here is the code for calculating entries of \mathcal{J} , \mathcal{T} matrices.

```
with(LinearAlgebra);
#Set up
pi := evalf(Pi);
E := evalf(exp(1));

#Unitary (replace it by E^((pi)/(p)I)for non-unitary case)
A := p -> I . (E^(1/2*I*pi/p));

#Quantum integer
nq := (p, n) -> (A(p)^(2*n) - A(p)^(-2*n))/(A(p)^2 - 1/A(p)^2);

#Quantum dimension
dq := (p, i) -> (-1)^i*nq(p, i + 1);

#Quantum factorial
fq := (p, n) -> evalf(product(nq(p, ii), ii = 1 .. n), 15);

#Admissible color
adm := (p, a, b, c) -> 'if'((a + b + c) mod 2 = 0 and
0 <= min(a + b - c, a - b + c, -a + b + c, 2*p - 4 - a - b - c), 1, 0);

#Quantum 3j symbol
trq := (p, a, b, c) -> 'if'(adm(p, a, b, c) = 1, evalf((-1)^(1/2*a+ 1/2*b + 1/2*c)
*fq(p, -1/2*a + 1/2*b + 1/2*c)*fq(p, 1/2*a - 1/2*b+ 1/2*c)*fq(p, 1/2*a + 1/2*b
- 1/2*c)*fq(p, 1/2*a + 1/2*b + 1/2*c + 1)/(fq(p, a)*fq(p, b)*fq(p, c)), 15), 0);
```

```

syq := (p, a1, a2, a3, a4, b1, b2, b3) -> fq(p, b1 - a1)*fq(p, b1 - a2)
*fq(p, b1 - a3)*fq(p, b1 - a4)*fq(p, b2 - a1)*fq(p, b2 - a2)*fq(p, b2 - a3)
*fq(p, b2 - a4)*fq(p, b3 - a1)*fq(p, b3 - a2)*fq(p, b3 - a3)*fq(p, b3 - a4)
*sum((-1)^z*fq(p, z + 1)/(fq(p, b1 - z)*fq(p, b2 - z)*fq(p, b3 - z)
*fq(p, z - a1)*fq(p, z - a2)*fq(p, z - a3)*fq(p, z - a4)), z = max(a1, a2,
a3, a4) .. min(b1, b2, b3));

#Quantum tetrahedron
Tet := (p, a, b, c, d, e, f) -> 'if'(adm(p, a, b, c)*adm(p, a, e, f)
*adm(p, c, d, e)*adm(p, b, d, f) = 1, evalf(syq(p, 1/2*a + 1/2*b + 1/2*c,
1/2*a + 1/2*e + 1/2*f, 1/2*c + 1/2*d + 1/2*e, 1/2*b + 1/2*d + 1/2*f, 1/2*a
+ 1/2*b + 1/2*d + 1/2*e, 1/2*a + 1/2*c + 1/2*d + 1/2*f, 1/2*b + 1/2*c + 1/2*e
+ 1/2*f)/(fq(p, a)*fq(p, b)*fq(p, c)*fq(p, d)*fq(p, e)*fq(p, f)), 15), 0);

#Quantum 6j symbol
sjq := (p, a, b, i, c, d, j) -> 'if'(adm(p, i, b, c)*adm(p, i, d, a)
*adm(p, c, j, d)*adm(p, b, j, a) = 1, evalf((-1)^i*nq(p, i + 1)
*Tet(p, i, b, c, j, d, a)/(trq(p, i, a, d)*trq(p, i, b, c)), 15), 0);

Fsjq := (p, a, b, i, c, d, j) -> (sqrt(((((((qd(p, j)) . (trq(p, b, c, i)))
. (trq(p, a, d, i))) . (1/dq(p, i))) . (1/trq(p, a, b, j)))
. (1/trq(p, c, d, j)))) . (sjq(p, a, b, i, c, d, j)));

Sjq := (p, a, b, i, c, d, j) -> 'if'(adm(p, i, b, c)*adm(p, i, d, a)
*adm(p, c, j, d)*adm(p, b, j, a) = 1, evalf((-1)^(i + j)*nq(p, i + 1)
*nq(p, j + 1)*Tet(p, i, b, c, j, d, a)/(trq(p, a, b, j)*trq(p, i, a, d)
*trq(p, i, b, c)), 15), 0);

# Twists, S-matrix entries, Global dimension and central charge
Tw := (p, a) -> (-1)^a*A(p)^(a*(a + 2));
Sm := (p, i, j) -> ((-1)^(i + j)) . (nq(p, (i + 1) . (j + 1)));
DD := p -> 'if'(p mod 2 = 1, add(nq(p, 2*i + 1)^2
, i = 0 .. 1/2*p - 3/2), add(nq(p, i + 1)^2, i = 0 .. p - 2));
P0 := p -> 'if'(p mod 2 = 1, add((Tw(p, 2.*i)) . (nq(p, 2*i + 1)^2)

```

```

, i = 0 .. 1/2*p - 3/2), add((Tw(p, i)) . (nq(p, i + 1)^2), i = 0 .. p - 2));
P1 := p -> 'if'(p mod 2 = 1, add((1/Tw(p, 2.*i)) . (nq(p, 2*i + 1)^2)
, i = 0 .. 1/2*p - 3/2), add((1/Tw(p, i)) . (nq(p, i + 1)^2), i = 0 .. p - 2));

#Quantum J coefficient.(unitary)
J := (p, f, e, d, c, b, a) -> 'if'(adm(p, a, b, c)
*adm(p, d, e, f) = 1, evalf(sqrt((-1)^(a + b + c + d + e + f)*nq(p, a + 1)
*nq(p, b + 1)*nq(p, c + 1)*nq(p, d + 1)*nq(p, e + 1)*nq(p, f + 1))
*add(Tw(p, b)*Tw(p, f)*add(Sjq(p, b, f, k, f, b, i)/Tw(p, i), i = 0 .. p - 2)
*add(Tw(p, j)*Sjq(p, d, c, k, c, d, j), j = 0 .. p - 2)
*Tet(p, k, d, e, f, f)*(-1)^k*Tet(p, c, a, b, b, k, c)/(Tw(p, d)*Tw(p, c)
*nq(p, k + 1)), k = 0 .. p - 2)/(trq(p, a, b, c)*trq(p, d, e, f)*DD(p)), 15), 0);

#Nonunitary
J1 := (p, f, e, d, c, b, a) -> 'if'(adm(p, a, b, c)
*adm(p, d, e, f) = 1, evalf(nq(p, a + 1)*nq(p, b + 1)*nq(p, c + 1)
*add(Tw(p, b)*Tw(p, f)*add(Sjq(p, b, f, k, f, b, i)/Tw(p, i), i = 0 .. p - 2)
*add(Tw(p, j)*Sjq(p, d, c, k, c, d, j), j = 0 .. p - 2)
*sjq(p, f, d, k, d, f, e)*trq(p, f, f, k)*trq(p, d, d, k)
*Tet(p, c, a, b, b, k, c)/(Tw(p, d)*Tw(p, c)*nq(p, k + 1)^2)
, k = 0 .. p - 2)/(trq(p, a, b, c)*trq(p, a, b, c)*DD(p)), 15), 0);

#Genus two T-matrix
T := (p, a, b, c) -> Tw(p, a)*Tw(p, b);

#computation for p=4 and 5
JJ1 := evalc(Re(Matrix(5, 5, [[J(5, 0, 0, 0, 0, 0, 0), J(5, 0, 0, 0, 0, 2, 2),
J(5, 0, 0, 0, 2, 0, 2), J(5, 0, 0, 0, 2, 2, 0), J(5, 0, 0, 0, 2, 2, 2)],
[J(5, 0, 2, 2, 0, 0, 0), J(5, 0, 2, 2, 0, 2, 2), J(5, 0, 2, 2, 2, 0, 2),
J(5, 0, 2, 2, 2, 2, 0), J(5, 0, 2, 2, 2, 2, 2)], [J(5, 2, 0, 2, 0, 0, 0),
J(5, 2, 0, 2, 0, 2, 2), J(5, 2, 0, 2, 2, 0, 2), J(5, 2, 0, 2, 2, 2, 0),
J(5, 2, 0, 2, 2, 2, 2)], [J(5, 2, 2, 0, 0, 0, 0), J(5, 2, 2, 0, 0, 2, 2),
J(5, 2, 2, 0, 2, 0, 2), J(5, 2, 2, 0, 2, 2, 0), J(5, 2, 2, 0, 2, 2, 2)],
[J(5, 2, 2, 2, 0, 0, 0), J(5, 2, 2, 2, 0, 2, 2), J(5, 2, 2, 2, 2, 0, 2),
J(5, 2, 2, 2, 2, 2, 0), J(5, 2, 2, 2, 2, 2, 2)]]]));

```

```

JJ2 := evalc(Re(Matrix(10, 10, [[J(4, 0, 0, 0, 0, 0, 0), J(4, 0, 0, 0, 0, 0, 1, 1),
J(4, 0, 0, 0, 0, 2, 2), J(4, 0, 0, 0, 1, 0, 1), J(4, 0, 0, 0, 1, 1, 0),
J(4, 0, 0, 0, 1, 1, 2), J(4, 0, 0, 0, 1, 2, 1), J(4, 0, 0, 0, 2, 0, 2),
J(4, 0, 0, 0, 2, 1, 1), J(4, 0, 0, 0, 2, 2, 0)], [J(4, 0, 1, 1, 0, 0, 0),
J(4, 0, 1, 1, 0, 1, 1), J(4, 0, 1, 1, 0, 2, 2), J(4, 0, 1, 1, 1, 0, 1),
J(4, 0, 1, 1, 1, 1, 0), J(4, 0, 1, 1, 1, 1, 2), J(4, 0, 1, 1, 1, 2, 1),
J(4, 0, 1, 1, 2, 0, 2), J(4, 0, 1, 1, 2, 1, 1), J(4, 0, 1, 1, 2, 2, 0)],
[J(4, 0, 2, 2, 0, 0, 0), J(4, 0, 2, 2, 0, 1, 1), J(4, 0, 2, 2, 0, 2, 2),
J(4, 0, 2, 2, 1, 0, 1), J(4, 0, 2, 2, 1, 1, 0), J(4, 0, 2, 2, 1, 1, 2),
J(4, 0, 2, 2, 1, 2, 1), J(4, 0, 2, 2, 2, 0, 2), J(4, 0, 2, 2, 2, 1, 1),
J(4, 0, 2, 2, 2, 2, 0)], [J(4, 1, 0, 1, 0, 0, 0), J(4, 1, 0, 1, 0, 1, 1),
J(4, 1, 0, 1, 0, 2, 2), J(4, 1, 0, 1, 1, 0, 1), J(4, 1, 0, 1, 1, 1, 0),
J(4, 1, 0, 1, 1, 1, 2), J(4, 1, 0, 1, 1, 2, 1), J(4, 1, 0, 1, 2, 0, 2),
J(4, 1, 0, 1, 2, 1, 1), J(4, 1, 0, 1, 2, 2, 0)], [J(4, 1, 1, 0, 0, 0, 0),
J(4, 1, 1, 0, 0, 1, 1), J(4, 1, 1, 0, 0, 2, 2), J(4, 1, 1, 0, 1, 0, 1),
J(4, 1, 1, 0, 1, 1, 0), J(4, 1, 1, 0, 1, 1, 2), J(4, 1, 1, 0, 1, 2, 1),
J(4, 1, 1, 0, 2, 0, 2), J(4, 1, 1, 0, 2, 1, 1), J(4, 1, 1, 0, 2, 2, 0)],
[J(4, 1, 1, 2, 0, 0, 0), J(4, 1, 1, 2, 0, 1, 1), J(4, 1, 1, 2, 0, 2, 2),
J(4, 1, 1, 2, 1, 0, 1), J(4, 1, 1, 2, 1, 1, 0), J(4, 1, 1, 2, 1, 1, 2),
J(4, 1, 1, 2, 1, 2, 1), J(4, 1, 1, 2, 2, 0, 2), J(4, 1, 1, 2, 2, 1, 1),
J(4, 1, 1, 2, 2, 2, 0)], [J(4, 1, 2, 1, 0, 0, 0), J(4, 1, 2, 1, 0, 1, 1),
J(4, 1, 2, 1, 0, 2, 2), J(4, 1, 2, 1, 1, 0, 1), J(4, 1, 2, 1, 1, 1, 0),
J(4, 1, 2, 1, 1, 1, 2), J(4, 1, 2, 1, 1, 2, 1), J(4, 1, 2, 1, 2, 0, 2),
J(4, 1, 2, 1, 2, 1, 1), J(4, 1, 2, 1, 2, 2, 0)], [J(4, 2, 0, 2, 0, 0, 0),
J(4, 2, 0, 2, 0, 1, 1), J(4, 2, 0, 2, 0, 2, 2), J(4, 2, 0, 2, 1, 0, 1),
J(4, 2, 0, 2, 1, 1, 0), J(4, 2, 0, 2, 1, 1, 2), J(4, 2, 0, 2, 1, 2, 1),
J(4, 2, 0, 2, 2, 0, 2), J(4, 2, 0, 2, 2, 1, 1), J(4, 2, 0, 2, 2, 2, 0)],
[J(4, 2, 1, 1, 0, 0, 0), J(4, 2, 1, 1, 0, 1, 1), J(4, 2, 1, 1, 0, 2, 2),
J(4, 2, 1, 1, 1, 0, 1), J(4, 2, 1, 1, 1, 1, 0), J(4, 2, 1, 1, 1, 1, 2),
J(4, 2, 1, 1, 1, 2, 1), J(4, 2, 1, 1, 2, 0, 2), J(4, 2, 1, 1, 2, 1, 1),
J(4, 2, 1, 1, 2, 2, 0)], [J(4, 2, 2, 0, 0, 0, 0), J(4, 2, 2, 0, 0, 1, 1),
J(4, 2, 2, 0, 0, 2, 2), J(4, 2, 2, 0, 1, 0, 1), J(4, 2, 2, 0, 1, 1, 0),
J(4, 2, 2, 0, 1, 1, 2), J(4, 2, 2, 0, 1, 2, 1), J(4, 2, 2, 0, 2, 0, 2),
J(4, 2, 2, 0, 2, 1, 1), J(4, 2, 2, 0, 2, 2, 0)]])]);

```

2. DATA AVAILABILITY STATEMENT

All data generated or analysed during this study are included in this article

REFERENCES

- [1] J. r. E. Andersen. Asymptotic faithfulness of the quantum $SU(n)$ representations of the mapping class groups. *Ann. of Math. (2)*, 163(1):347–368, 2006.
- [2] J. r. E. Andersen, G. Masbaum, and K. Ueno. Topological quantum field theory and the Nielsen-Thurston classification of $M(0, 4)$. *Math. Proc. Cambridge Philos. Soc.*, 141(3):477–488, 2006.
- [3] G. Belletti, R. Detcherry, E. Kalfagianni, and T. Yang. Growth of quantum $6j$ -symbols and applications to the volume conjecture. *J. Differential Geom.*, 120(2):199–229, 2022.
- [4] J. S. Birman. *Braids, links, and mapping class groups*. Annals of Mathematics Studies, No. 82. Princeton University Press, Princeton, N.J.; University of Tokyo Press, Tokyo, 1974.
- [5] C. Blanchet, N. Habegger, G. Masbaum, and P. Vogel. Three-manifold invariants derived from the Kauffman bracket. *Topology*, 31(4):685–699, 1992.
- [6] C. Blanchet, N. Habegger, G. Masbaum, and P. Vogel. Topological quantum field theories derived from the Kauffman bracket. *Topology*, 34(4):883–927, 1995.
- [7] W. Bloomquist and Z. Wang. On topological quantum computing with mapping class group representations. *J. Phys. A*, 52(1):015301, 23, 2019.
- [8] P. Bruillard, S.-H. Ng, E. C. Rowell, and Z. Wang. On classification of modular categories by rank. *Int. Math. Res. Not. IMRN*, 2016(24):7546–7588, 2016.
- [9] A. Cappelli, C. Itzykson, and J.-B. Zuber. Modular invariant partition functions in two dimensions. *Nuclear Phys. B*, 280(3):445–465, 1987.
- [10] P. de la Harpe. *Topics in geometric group theory*. Chicago Lectures in Mathematics. University of Chicago Press, Chicago, IL, 2000.
- [11] R. Detcherry and E. Kalfagianni. Quantum representations and monodromies of fibered links. *Adv. Math.*, 351:676–701, 2019.
- [12] B. Farb and D. Margalit. *A primer on mapping class groups*, volume 49 of *Princeton Mathematical Series*. Princeton University Press, Princeton, NJ, 2012.
- [13] M. H. Freedman, K. Walker, and Z. Wang. Quantum $SU(2)$ faithfully detects mapping class groups modulo center. *Geom. Topol.*, 6:523–539, 2002.
- [14] L. Funar. On the TQFT representations of the mapping class groups. *Pacific J. Math.*, 188(2):251–274, 1999.
- [15] P. M. Gilmer and G. Masbaum. Maslov index, lagrangians, mapping class groups and TQFT. *Forum Math.*, 25(5):1067–1106, 2013.
- [16] F. M. Goodman, P. de la Harpe, and V. F. R. Jones. *Coxeter graphs and towers of algebras*, volume 14 of *Mathematical Sciences Research Institute Publications*. Springer-Verlag, New York, 1989.

- [17] D. Johnson. Spin structures and quadratic forms on surfaces. *J. London Math. Soc. (2)*, 22(2):365–373, 1980.
- [18] V. F. R. Jones. Index for subfactors. *Invent. Math.*, 72(1):1–25, 1983.
- [19] V. F. R. Jones. Hecke algebra representations of braid groups and link polynomials. *Ann. of Math. (2)*, 126(2):335–388, 1987.
- [20] L. H. Kauffman and S. L. Lins. *Temperley-Lieb recoupling theory and invariants of 3-manifolds*, volume 134 of *Annals of Mathematics Studies*. Princeton University Press, Princeton, NJ, 1994.
- [21] M. Kontsevich and A. Zorich. Connected components of the moduli spaces of Abelian differentials with prescribed singularities. *Invent. Math.*, 153(3):631–678, 2003.
- [22] C. J. Leininger. On groups generated by two positive multi-twists: Teichmüller curves and Lehmer’s number. *Geometry & Topology*, 8(3):1301–1359, 2004.
- [23] W. B. R. Lickorish. Skeins and handlebodies. *Pacific J. Math.*, 159(2):337–349, 1993.
- [24] Z. Liu and F. Xu. Jones-Wassermann subfactors for modular tensor categories. *Adv. Math.*, 355:106775, 40, 2019.
- [25] G. Masbaum. An element of infinite order in TQFT-representations of mapping class groups. In *Low-dimensional topology (Funchal, 1998)*, volume 233 of *Contemp. Math.*, pages 137–139. Amer. Math. Soc., Providence, RI, 1999.
- [26] G. Masbaum and J. D. Roberts. On central extensions of mapping class groups. *Math. Ann.*, 302(1):131–150, 1995.
- [27] G. Masbaum and P. Vogel. 3-valent graphs and the Kauffman bracket. *Pacific J. Math.*, 164(2):361–381, 1994.
- [28] H. Masur and S. Tabachnikov. Rational billiards and flat structures. In *Handbook of dynamical systems, Vol. 1A*, pages 1015–1089. North-Holland, Amsterdam, 2002.
- [29] C. T. McMullen. Prym varieties and Teichmüller curves. *Duke Math. J.*, 133(3):569–590, 2006.
- [30] M. Mignard and P. Schauenburg. Modular categories are not determined by their modular data. *Lett. Math. Phys.*, 111(3):Paper No. 60, 9, 2021.
- [31] S.-H. Ng and P. Schauenburg. Congruence subgroups and generalized Frobenius-Schur indicators. *Comm. Math. Phys.*, 300(1):1–46, 2010.
- [32] N. Reshetikhin and V. G. Turaev. Invariants of 3-manifolds via link polynomials and quantum groups. *Invent. Math.*, 103(3):547–597, 1991.
- [33] J. Roberts. Skeins and mapping class groups. *Math. Proc. Cambridge Philos. Soc.*, 115(1):53–77, 1994.
- [34] E. Rowell, R. Stong, and Z. Wang. On classification of modular tensor categories. *Comm. Math. Phys.*, 292(2):343–389, 2009.
- [35] W. P. Thurston. On the geometry and dynamics of diffeomorphisms of surfaces. *Bull. Amer. Math. Soc. (N.S.)*, 19(2):417–431, 1988.
- [36] V. G. Turaev. *Quantum invariants of knots and 3-manifolds*, volume 18 of *de Gruyter Studies in Mathematics*. Walter de Gruyter & Co., Berlin, 1994.
- [37] V. G. Turaev. *Quantum invariants of knots and 3-manifolds*, volume 18 of *De Gruyter Studies in Mathematics*. Walter de Gruyter & Co., Berlin, revised edition, 2010.

- [38] W. A. Veech. Teichmüller curves in moduli space, Eisenstein series and an application to triangular billiards. *Invent. Math.*, 97(3):553–583, 1989.
- [39] B. Wajnryb. A simple presentation for the mapping class group of an orientable surface. *Israel J. Math.*, 45(2-3):157–174, 1983.
- [40] Z. Wang. *Topological quantum computation*, volume 112 of *CBMS Regional Conference Series in Mathematics*. Published for the Conference Board of the Mathematical Sciences, Washington, DC; by the American Mathematical Society, Providence, RI, 2010.
- [41] H. Wenzl. On sequences of projections. *C. R. Math. Rep. Acad. Sci. Canada*, 9(1):5–9, 1987.
- [42] E. Witten. Quantum field theory and the Jones polynomial. *Comm. Math. Phys.*, 121(3):351–399, 1989.
- [43] A. Wright. Translation surfaces and their orbit closures: an introduction for a broad audience. *EMS Surv. Math. Sci.*, 2(1):63–108, 2015.
- [44] A. Zorich. Flat surfaces. In *Frontiers in number theory, physics, and geometry. I*, pages 437–583. Springer, Berlin, 2006.

Email address: ryz22@mails.tsinghua.edu.cn